

Surface functionalization through adsorption of organic molecules

This article has been downloaded from IOPscience. Please scroll down to see the full text article.

2007 J. Phys.: Condens. Matter 19 305018

(<http://iopscience.iop.org/0953-8984/19/30/305018>)

View [the table of contents for this issue](#), or go to the [journal homepage](#) for more

Download details:

IP Address: 129.252.86.83

The article was downloaded on 28/05/2010 at 19:51

Please note that [terms and conditions apply](#).

Surface functionalization through adsorption of organic molecules

Arrigo Calzolari and Rosa Di Felice

Center on nanoStructures and bioSystems at Surfaces of INFM-CNT (S³), c/o Dipartimento di Fisica, Università di Modena e Reggio Emilia, Via Campi 213a, 41100 Modena, Italy

E-mail: calzolari.arrigo@unimore.it

Received 5 February 2007, in final form 1 March 2007

Published 13 July 2007

Online at stacks.iop.org/JPhysCM/19/305018

Abstract

We report a first-principles study about the structural and electronic properties of two hybrid organic-molecule/inorganic-surface interfaces. We consider the adsorption of cysteine amino acids on Au(111) and of styrene molecules on the dimerized Si(100)-(2 × 1) surface, as prototypical systems for the functionalization of both metallic and semiconducting substrates. We focus on the adsorption mechanisms at the submonolayer regime, that we describe in terms of molecule/surface and molecule/molecule interactions. In both cases, our results show a strong electronic mixing and the formation of hybrid bonding states at the interface.

(Some figures in this article are in colour only in the electronic version)

Introduction

The enormous development of surface science is mainly motivated by the simple observation that the interactions between an object and the external world occur through its surface. Thus, the study of solid-state surfaces allows one both to characterize the intrinsic properties of the external layers of a material and to figure out its behaviour in the presence of external agents, such as atoms, molecules, clusters or further surfaces [1].

Particular attention has been devoted to the fabrication and the manipulation of nanostructures at surfaces. In this sense, the revolutionary advent of some chemical techniques (e.g. Langmuir–Blodgett), as well as of the microscopies (e.g. AFM/STM) and of the nanolithographies (dip-pen, UHV nanoprinting), has opened the way to the possibility of depositing atoms and molecules on surfaces in a controlled way [2].

The adsorption of single atoms and small inorganic molecules (H₂, O₂, etc) was traditionally related to processes such as passivation, oxidation and epitaxial growth of the surfaces. More recently, the functionalization of surfaces with organic molecules [3] has attracted a tremendous interest in view of novel nanoscale applications, namely the

nanopatterning of surfaces, the realization of self-assembled monolayers, the control of the early stage processes for the deposition of further materials (thin and thick film growth), and the anchorage and the docking of large macromolecules (nucleic acids, proteins and cells).

Particularly appealing are, in fact, some intrinsic properties of the organic molecules such as self-aggregation, self-recognition, and the possibility of easily changing the structural, electronic and reactive properties by modifying a few selected functional groups. Despite their simplicity, small organic/bio molecules (e.g. alkanethiols, aromatic rings, metallo-porphyrines, nucleobases or amino acids) display peculiar quantum properties due to their low dimensionality, i.e. related to the nature of the single chemical bonds and the coordination number.

Clearly, the effects of the surface functionalization depend on the choice of the starting surface and the adsorbed molecule, and a huge variety of different interfaces may be realized. However, we can roughly consider two broad classes of hybrid systems based on (i) metallic and (ii) semiconducting surfaces.

The study of metal/molecule interfaces has been strongly motivated by the expectation of realizing new forms of electronics, in which nanoscale objects and molecular devices replace the transistors of today's silicon technology. These 'concept devices' are based on hybrid metal/molecule/metal interfaces, where molecules are the active element of the device, while the metal pads constitute both the structural support for the molecule and the leads of the circuit. On the other hand, the functionalization of semiconductor surfaces allows one to obtain nanostructured materials, whose properties may be tuned in controlled ways. The localized and directional character of semiconductor bonds at surfaces is able to impart an ordered arrangement to the adsorbed molecules, making the substrate an intrinsic template for the growth of the molecular layer.

In both cases, a deep understanding of these molecular nanostructures and their coupling with surfaces requires a microscopic description of the system. In this paper we report a state-of-the-art study of the structural and electronic properties of hybrid interfaces, based on *ab initio* density functional theory (DFT) calculations. We consider two key examples of organic molecules on metallic and semiconducting surfaces, i.e. cysteine/Au(111) [4, 5] and styrene/Si(100) [6], in the submonolayer coverage regime. We show the complex interactions at the interface, focusing on the coupling between the adlayer and the substrate, and on its effects on the electronic and transport properties of the systems.

1. Method

Our calculations were performed in the framework of plane-wave density functional theory (DFT) [7] with the gradient-corrected PW91 exchange–correlation functional [8], as implemented in the PWSCF package [9].

In the DFT functional, the electron–ion interactions were described by *ab initio* norm-conserving and ultrasoft pseudopotentials [10, 11]. Only the valence electrons were explicitly taken into account for all the species, whereas the inner shells were part of the frozen cores. For Au, the semicore 5d electrons were also included in the DFT functional. The accuracy of the plane-wave kinetic energy cutoff (22 Ryd for metal and 20 Ryd for semiconducting substrate) and of Brillouin zone sums [12] was carefully checked [4, 6, 13]. The structures were relaxed until the forces on all atoms were lower than 0.03 eV \AA^{-1} .

Cysteine/Au(111) interfaces were modelled using repeated supercells consisting of four (111) layers of gold atoms, one cysteine molecule adsorbed at one surface of the slab, and a vacuum width of $\sim 10 \text{ \AA}$. Each layer of the slab had 12 gold atoms forming a $(3 \times 2\sqrt{3})$

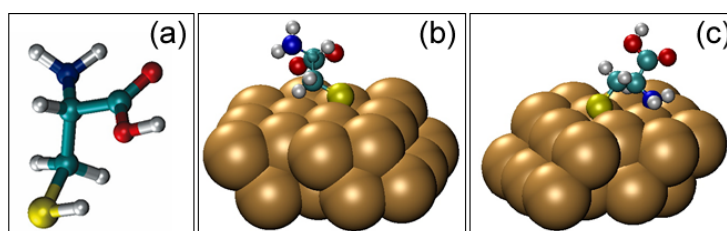


Figure 1. (a) Atomic structure of cysteine in the molecular form, with the S atom (largest sphere) saturated by H. (b), (c) 3D representations of the two studied configurations for the radical cysteine adsorbed on the Au(111) surface. The S headgroup of cysteine is adsorbed at the twofold lattice bridge site, with the NH_2 group participating (b) or not (c) in cysteine-gold bonding; in both cases the $\text{S}-\text{C}_\beta$ bond is oriented at about 60° from the surface normal.

two-dimensional (2D) supercell with a surface area of $(10.14 \times 8.78) \text{ \AA}^2$. The density of adsorbed cysteines was about half the experimental density for ‘wet’ monolayers, where a $(3\sqrt{3} \times 6)\text{R}30$ unit cell with the fingerprints of six cysteine adsorbates was observed [14].

Styrene/Si(100) interfaces were studied in two limiting coverage regimes: the single molecule and the full monolayer configuration. In both cases we simulated the surface using periodically repeated supercells containing six atomic layers and $\sim 16 \text{ \AA}$ of vacuum. Styrene was adsorbed onto one surface of the slab, while the other side was passivated with a monolayer of hydrogen atoms. The (2×1) reconstruction of Si(100) was simulated with different lateral periodicity, depending on the coverage: a large $c(16 \times 16)$ cell was used in the case of single molecule adsorption to isolate molecules in neighbouring cells; and a $p(2 \times 2)$ cell was used in the case of monolayer configurations.

2. Organic-molecule/metal-surface interface

Organic molecules and biomolecules with a sulfur headgroup are attracting considerable interest because of their wide use in nanotechnology-related fields, like surface patterning and functionalization [15–17] and molecular electronics [18, 19]. Among the several interesting applications, the strong affinity of sulfur to different metals can be exploited to form contacts, to link other species to a supporting metallic surface, or to form well-ordered self-assembled monolayers (SAMs) [15]. In biomolecules, the S-containing cysteine amino acid (figure 1(a)) is especially interesting because, being often located on the border of large proteins, it can provide a link to anchor these proteins to inorganic supports.

Since the S group is commonly retained to have a strong affinity for metals, our first interest was to understand the strength and mechanisms of the resulting bonds obtained by exploiting only the thiol group of cysteine for attachment to a Au(111) surface. However, in a variety of cysteine/metal interaction conditions the radical can employ one or more functional groups to couple to metal ions or surfaces [20–22]. Thus we also wanted to understand the relative strength of cysteine/gold bonds obtained with multiple (thiol and amino) functional groups. The two adsorbate geometries that have been examined are depicted in figure 1. In the following, we will refer to the cysteine/Au(111) interfaces of figures 1(b) and (c) as thiolate and amino-thiolate respectively. In both cases, cysteine is adsorbed on a gold surface in the radical form, i.e. losing the H atom bonded to S, which is thus free to coordinate with the outermost substrate atoms.

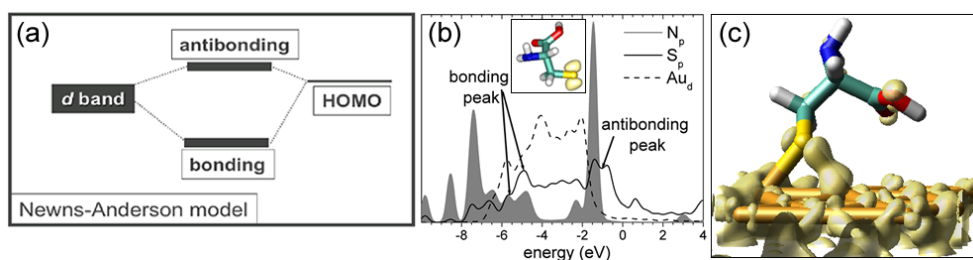


Figure 2. (a) Scheme of the Newns–Anderson model for *molecular* chemisorption at transition metal surfaces. DOS (b) and selected electron state (c) of the thiolate cysteine/Au(111) interface, with the S headgroup at the twofold coordination site. The inset in panel (b) shows the isosurface plot of the radical HOMO, that participates in bonding with gold orbitals. In the DOS plot, the origin of the energy scale is set at the system Fermi level: the Fermi level crosses the S_p – Au_d antibonding peaks in a region of low but non-negligible DOS.

2.1. Cysteine on Au(111): thiolate bond

In this section, we discuss the electronic mechanisms that govern the S–Au coupling for the system in which the cysteine/Au(111) interface is realized by thiolate bonds only (figure 1(b)). When the thiol group of cysteine is the unique anchor to the surface, there is a multiplicity of possible metastable configurations defined by the adsorption location of the S atom on the substrate lattice. Our results [4, 5] are in line with state-of-the-art DFT computational data [13, 23, 24] for methyl-thiol/Au(111) in a high-coverage regime: the thiol group selects a twofold coordination at a bridge location between two Au atoms of the surface, slightly displaced towards the threefold fcc site (figure 1). The energetically favourable equilibrium geometry shows that internal bond lengths and angles in the adsorbed radical remain very similar to the gas-phase conformation [4, 5].

For the thiolate interface of figure 1(b), we computed the full electronic structure, which allowed us to interpret the adsorption mechanisms and discriminate between chemisorption and physisorption. The high adsorption energy of 0.77 eV/molecule (with respect to gas-phase cysteine) is already an indication of bond formation. In addition, we find both bonding and antibonding mixed S–Au orbitals. The picture that we deduce conforms to the Newns–Anderson chemisorption model [2]. This scheme is usually adopted to describe the electronic hybridization occurring upon atomic chemisorption on metal surfaces: it predicts that the interaction of a localized orbital on the adsorbate mixes with the narrow d band of the metal, thus producing hybrid orbitals of both bonding and antibonding nature, below and above the centre of the metal d band, respectively [2]. In the case of an atomic adsorbate, it is the highest electron level that interacts with the substrate d band; in the case of a molecular adsorbate, the adsorbate level responsible for coupling with the metal orbitals is the highest occupied molecular orbital (HOMO). A pictorial representation of this mechanism is shown in figure 2(a). The rationale is that the narrow d band, as opposed to the widely dispersed s band, behaves in practice as an effective energy level that couples with the highest occupied adsorbate level, thus producing bonding and antibonding energy states. Due to the presence of the underlying metal s band, the bonding and antibonding hybrids are not single levels but manifolds that originate spread peaks in the density of states (DOS) [4, 2], as shown in figure 2.

Figure 2(b) shows the DOS projected onto Au_d , S_p , N_p orbitals, rescaled to the number of orbitals contributing for each atomic species, to make the N and S signals visible with respect to the major Au background. The energy range between approximately -6 and -2 eV marks the Au d band. The two S peaks (solid line) at the highest and lowest edges of this range

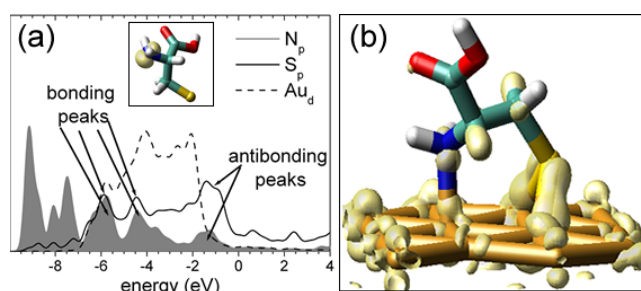


Figure 3. DOS (a) and selected electron state (b) of the amino-thiolate cysteine/Au(111) interface, with the S headgroup at the twofold coordination site and the N atom of the amino fragment approximately on top of a substrate Au atom. In the DOS plot, the Fermi level is the origin of the energy scale.

are attributed to the antibonding and bonding features, respectively, in line with the Newns–Anderson model. This mechanism is verified by showing an isosurface plot (figure 2(c)) of a representative orbital that contributes to the bonding peak (similar states are present also for the antibonding peak): several other electron states of the same kind constitute the peaks centred around -5 and -1 eV in the S_p DOS in figure 2(b). It is remarkable that the antibonding peak for this system is partially occupied: in fact, it is crossed by the Fermi level. This resulting electronic structure, along with the significant energy gain upon cysteine adsorption on Au(111) in the thiolate form, indicates a strong driving force towards the chemisorption reaction.

2.2. Cysteine on Au(111): amino-thiolate bond

Our next interest was in addressing whether the lone pair of the amino group also takes part in the adsorption reaction, as suggested by recent investigations [22]. On the basis of the relative formation energy between the thiolate (figure 1(b)) and amino-thiolate (figure 1(c)) cysteine/Au(111) interfaces, in favour of the latter by ~ 0.48 eV/molecule, our results indicate that the preferred bonding conformation for cysteine on Au(111) involves both the thiol and the amino functional groups. Also, for the amino-thiolate interface, the intramolecular bond lengths and bond angles remain very close to the values pertaining to gas-phase cysteine. Despite the higher stability of the amino-thiolate conformation for the cysteine/Au(111) interface, we note that the possibility of exploiting the amino group to bind the molecule to the metal surface is plausibly hindered in most cases where cysteine is the anchoring group of polypeptides or proteins to surfaces [21], because the NH_2 fragment is engaged in peptide bonds. Therefore, we expect that macromolecules that can bind to a Au(111) surface through a cysteine would do that by exploiting only the thiol fragment.

We then investigated whether the adsorption mechanism is profoundly changed with respect to the Newns–Anderson model explained above, when anchoring through the thiol is altered by the involvement of the NH_2 portion. The electronic properties of the amino-thiolate interface are illustrated in figure 3: the shadowed area, the solid line, the dashed line, represent the DOS projection onto the atomic orbitals. One can see immediately that the strong N peak present in the thiolate interface (figure 2(b)) at around -1.3 eV, due to the molecular nitrogen lone pair, is depressed in the amino-thiolate interface: this is a clear indication that the N lone pair is modified. In figure 3 we find again bonding and antibonding peaks, indicative of the Newns–Anderson chemisorption model. The isosurface plot shown in figure 3(b) indicates that the N lone pair (shown in the inset for the cysteine radical phase) gives a contribution to these

peaks. Thus, the cysteine–gold coupling mechanism remains consistent with the chemisorption model, only quantitatively changed by the role of the amino group. The antibonding peak is still crossed by the Fermi level (origin of the energy scale).

2.3. Cysteine on Au(111): discussion

The basic concept that we underline from the above description of the cysteine–gold coupling is that the available cysteine functional groups are very reactive, and in particular the S handle is the strongest binding part of the amino acid. The prevalent contribution to the energy gain upon formation of the hybrid interface comes from the S–Au coupling (2.03 eV/molecule); then some more energy is gained with the additional N–Au coupling (0.26 eV/molecule). In addition, we remark that, independently of the adsorption configuration among those reported above, the S–Au coupling always occurs in the thiolate form. With these results at hand, we can qualitatively compare our findings to what is known about this system from experimental studies. Most early experiments were focused on the detection of the adsorption geometry and in particular long-range order [14]. We did not try to predict the two-dimensional order, because this property might be strongly affected by the DFT approximations: lateral cysteine–cysteine interactions are likely controlled by dispersion forces. Alternatively, we chose geometries compatible with observations in terms of lateral reconstructions and molecular coverage [14], and focused on the electronic structure to investigate molecule–metal hybridization. Rigorous experiments to investigate the electronic properties of cysteine/gold interfaces, with focus on understanding the nature of the S–Au affinity, appeared only recently both in ultra-high-vacuum [25, 26] and vapour [27] deposition ambient on different Au faces. Through the analysis of sulfur core-level shifts by x-ray photoemission, the existence of the thiolate bond was proven, along with another S species that is ascribed to atomic S after S–C bond cleavage in the molecule [25]. Thus, although an exact comparison between measured and computed quantities is not feasible (core-level shifts are elusive to pseudopotential calculations), we can definitely claim a reproducible qualitative agreement about the nature of the molecule–metal binding.

3. Organic-molecule/semiconductor-surface interface

Silicon surfaces and interfaces have been widely investigated [28], because of their fundamental and technological application in conventional devices. However, the functionalization of the Si surfaces through the adsorption of organic molecules allows one to handle the intrinsic properties of the substrate, paving the way to obtain novel materials with desired properties, which may be exploited for nanotechnology (nanoelectronics, nonlinear optics, optoelectronics, etc), and bioengineering applications (sensors, molecular recognition, etc) [29].

Since the surface reactivity is essentially ruled by the presence of unsaturated orbitals at the surface, most experiments were done using hydrogen-terminated Si substrates [30, 31]. The passivated surfaces prevent spurious oxidation processes, but require further dynamical mechanisms to abstract a hydrogen atom and allow the deprotected Si dangling bond to react with the organic molecule [32, 33].

On the other hand, the clean Si(100) surface exhibits an ordered arrangement of Si=Si dimer rows, that may easily react with the carbon–carbon double bond (C=C) of most organic molecules, as demonstrated by recent experiments exploiting unsaturated hydrocarbons (e.g. ethylene, benzene, cyclopentene, etc) [34, 35]. Moreover, the direct measurement of the transport properties through a single molecule on Si(100) has recently validated the possibility of realizing functioning semiconductor-based molecular devices [36, 37]. In particular,

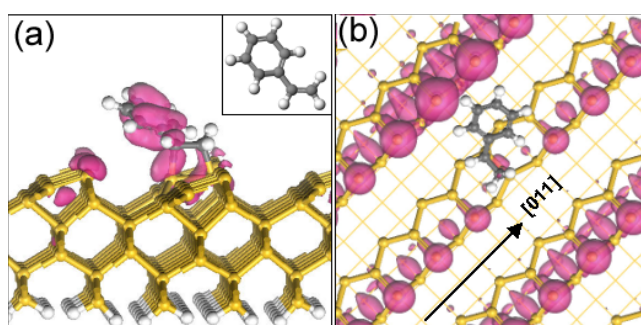


Figure 4. Single styrene molecule adsorbed on a Si(100)-(2 × 1) surface. (a) Isosurface plot of a hybrid Si–C bonding state. (side view). (b) Isosurface plot of the resulting HOMO state for the adsorbed system (top view). The state is strongly reminiscent of the HOMO state of the clean surface. The inset shows an isolated styrene molecule. The arrow marks the direction of the Si=Si dimer rows.

the deposition of styrene molecules on Si(100) is a representative model, since styrene is constituted of two building blocks (inset of figure 4), i.e. the phenyl ($-\text{C}_6\text{H}_5$) and the vinyl ($-\text{CH}=\text{CH}_2$) groups, that are the key components of most conjugated molecular structures and organic polymers.

3.1. Styrene on Si(100): single molecule

Our results for the clean Si(100)-(2 × 1) surface reproduce well the existing experimental [28] and theoretical [38] results: the external atomic layer undergoes a strong reconstruction forming ordered rows of double-bonded Si=Si dimers along the [011] direction (see figure 1). The dimers are tilted, due to a charge transfer from the ‘down’ to the ‘up’ atom. Accordingly, the lowest unoccupied molecular orbital (LUMO) and the highest occupied molecular orbital (HOMO) are surface states, localized around the ‘down’ and the ‘up’ atom respectively. The corresponding density of states (figure 5(a)) is characterized by a small energy gap, caused by the presence of such surface states in the original Si gap.

On the basis of experimental evidences [36, 39, 40] the starting configuration for our *ab initio* relaxation was obtained by orienting the vinyl group of styrene almost parallel to one Si=Si dimer. The adsorption process leads to an energy gain of 1.64 eV/molecule, against a local atomic relaxation only around the adsorption site. The styrene molecule and the surface do not exhibit relevant distortions, except for the very dimer beneath the molecule that fully derelaxes, removing the original tilting angle (see figure 4(a)).

The chemisorption may be described in terms of the so-called [2 + 2] cycloaddition reaction [35]: the double bonds of the vinyl group ($\text{C}=\text{C}$) and of the Si=Si dimer beneath break to form a fourfold ring of single bonds Si–Si–C–C. The formation of Si–C bonds implies a uniform charge redistribution, which removes the buckling of the clean dimer. Since the binding mechanism involves the vinyl group and a single dimer, the counter-relaxation occurs very locally at the adsorption site, leaving the rest of the surface, as well as the phenyl group, almost unperturbed.

This interpretation is confirmed by the analysis of the electronic structure. By comparing the densities of states of the system before (figure 5(a)) and after (figure 5(b)) the adsorption of a single molecule, we can identify the effects induced by the presence of the styrene.

The projection on the molecular states (shaded area) primarily affects the low-energy range of the spectrum, adding new peaks to the original Si DOS. The rest of the spectrum

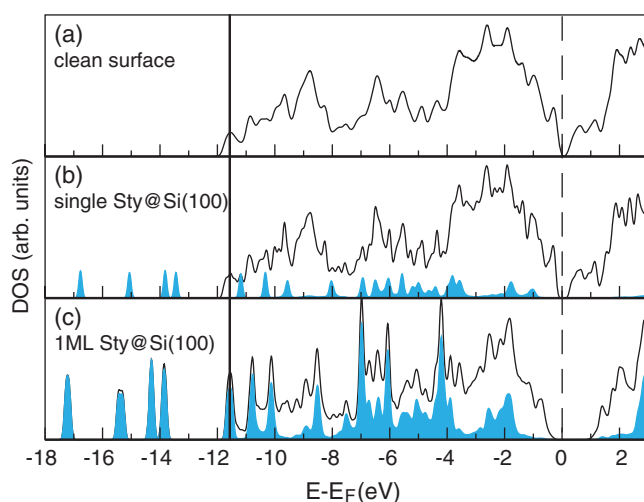


Figure 5. (a) Clean Si(100)-(2 × 1) surface, (b) single-molecule/Si(100) interface, (c) styrene adsorption on Si(100) at 1 monolayer (1 ML) coverage. Black lines identify the total DOS, the shaded area the corresponding projections on styrene molecules. The zero-energy reference is set to the Fermi level of each system (vertical dashed line). Straight vertical lines mark the bottom edge of the silicon bands.

(e.g. between the vertical lines) maintains the features of the clean surface. In particular, the HOMO state of the adsorbed system (figure 4(b)) reproduces the characteristics of the corresponding HOMO state of the clean surface (i.e. localized on the upper part of the tilted dimer). The [2 + 2] cycloaddition reaction introduces new Si–C bonding states at -1.0 eV, as shown in (figure 4(a)). The corresponding antibonding orbitals are also detected in the empty part of the spectrum (not shown) [6]. As regards the case of the adsorption of a single molecule, we conclude that the molecule is strongly chemisorbed on top of the surface. However, since the reaction involves only a single dimer (1 out of 16 in our simulation), the adsorption of a single molecule does not significantly modify the overall electronic properties of the surface around the Fermi energy.

3.2. Styrene on Si(100): full monolayer

We then turn our interest to the adsorption of styrene molecules at the saturation coverage of 1 monolayer (1 ML), which corresponds to one styrene for every surface dimer. Experimental observations [15, 16, 34] show that the spatial arrangement of self-assembled monolayers (SAMs) may be strongly affected by non-bonding interactions such as van der Waals (VdW) forces. Since standard DFT does not include these effects, we used the well-established polymer consistent force field (PCFF) [41] to reach the equilibrium structures. The starting atomic configurations at 1 ML coverage were obtained by saturating each Si=Si dimer with a styrene molecule. We first optimized the structure at the PCFF level (which treats electrostatic and VdW interactions), and then calculated the corresponding electronic structure at the DFT level, keeping the atoms fixed at the relaxed geometry.

In agreement with the experimental data [40], our resulting overlayer is highly ordered and oriented along the dimer rows, with a intermolecular distance of 3.8 Å along the [011] direction, induced by the substrate periodicity (see figure 6). The phenyl groups arrange in a parallel fashion, almost vertically with respect to the Si surface.

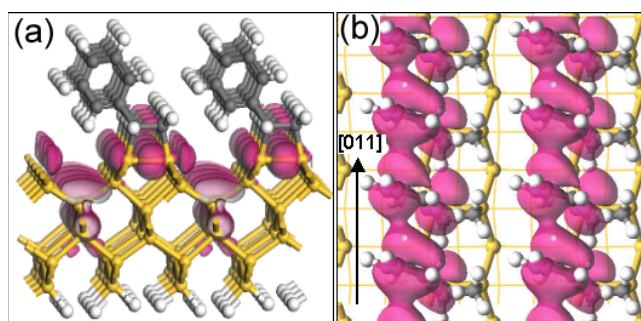


Figure 6. Styrene molecule adsorbed on a Si(100)-(2 × 1) surface at 1 ML coverage. (a) Isosurface plot of a hybrid Si–C bonding state (side view). (b) Isosurface plot of π – π orbitals delocalized through the phenyl groups along the dimer direction (top view). The arrow marks the direction of the original Si=Si dimer rows.

As for the previous case, the adsorption mechanism may be referred to the [2 + 2] cycloaddition reaction, through the formation of a four-membered ring for each adsorbed molecule and the derelaxation of every Si dimer. For each vinyl/dimer pair, we can identify hybrid Si–C bonding (antibonding) states (figure 6(a)) similar to those relative to the single-molecule adsorption (figure 4(a)). On the other hand, the complete saturation of the Si=Si surface dimers leads to dramatic effects on the conduction properties of the overall interface (see figure 5(c)). In the monolayer configuration, the frontier peaks (e.g. the HOMO and the LUMO) disappear, leading to a depletion of states that enlarges the band gap. In fact, the formation of the Si–C bonds—energetically more stable than the Si=Si double bond—is responsible for the saturation of the Si surface states, which are shifted away from the gap, towards the continuum of states of bulk silicon. We conclude that it is possible to tune the bandgap of the interface (and therefore its conduction properties) in a programmable way, controlling the dosage of the adsorbed molecules [6].

We finally analysed the effects of the molecule–molecule interactions. Passing from the single styrene to the monolayer configuration we observe (figures 5(b), (c)) a downward shift of the low energy peaks ($E < -12.0$ eV) and the broadening of the peaks deriving from the aromatic ring. The former effect is due to the electrostatic interaction among the molecules in this close-packed configuration. The latter is a signature of the π – π interaction between the assembled molecules, tending to create delocalized orbitals at the surface, as shown in figure 6(b). The π channels expand parallel to the dimer rows, while they are almost localized in the perpendicular direction. This implies that the directional Si=Si motif of the clean surface also drives the formation of an ordered pattern of one-dimensional electronic wires on top of the surface.

4. Conclusions

In this paper we presented two key systems, cysteine/Au(111) and styrene/Si(100), representing the adsorption of small organic molecules on both metallic and semiconducting surfaces. In both cases, the molecules strongly interact with the substrate, forming hybrid molecule/substrate bonding (antibonding) orbitals, being the signature of a chemisorption reaction. The details of the adsorption mechanism depend on the details of the single constituents of the interface. In particular, they can be referred to the Newns–Anderson model (i.e. HOMO–d band interaction) and the [2 + 2] cycloaddition (i.e. double bond–double interaction) for the thiolated and vinylated systems, respectively.

We conclude by mentioning that molecular chemisorption is not the only possible scenario for molecules on surfaces: physisorbed or intermediated configurations have been experimentally observed and theoretically predicted in different organic molecule/surface systems (e.g. Cu(II)-phthalocyanine/Au(111), pentacene/Cu(100) [42]). Therefore, if on one hand the molecular functionalization of surfaces represents a powerful tool to handle the properties of the inorganic materials, on the other hand the huge variety of possible molecule/substrate interactions prevents one from determining *a priori* the final properties of the overall interface.

Acknowledgments

Andrea Ferretti, Alice Ruini, Marilia J Caldas, Annabella Selloni and Elisa Molinari are gratefully acknowledged for fruitful collaborations. Funding was provided in part by the Regional Laboratory of Emilia-Romagna 'Nanofaber'; and by the EC through contracts IST-2000-28024 and IST-2001-38951. Computing time at the CINECA supercomputing facilities was provided by INFN-CNR.

References

- [1] Holloway S and Richardson N V (ed) 2000 *Handbook of Surface Science* (Amsterdam: North-Holland, Elsevier)
- [2] Hammer B and Nørskov J K 1997 Theory of adsorption and surface reactions *Chemisorption and Reactivity of Supported Clusters and Thin Films* ed R M Lambert and G Pacchioni (Dordrecht: Kluwer–Academic) pp 285–351
- [3] Yates J T Jr 1998 *Science* **279** 335
- [4] Di Felice R, Selloni A and Molinari E 2003 *J. Phys. Chem. B* **107** 1151
- [5] Di Felice R and Selloni A 2004 *J. Chem. Phys.* **120** 4906
- [6] Calzolari A, Ruini A, Molinari E and Caldas M J 2006 *Phys. Rev. B* **73** 125420
- [7] Dreizler R M and Gross E K U 1990 Density functional theory *An Approach to the Quantum Many Body Problem* (Berlin: Springer)
- [8] Perdew J P, Chevary J A, Vosko S H, Jackson K A, Singh D J and Fiolhais C 1992 *Phys. Rev. B* **46** 6671
- [9] Baroni S, De Gironcoli S, Dal Corso A and Giannozzi P <http://www.pwscf.org>
- [10] Troullier N and Martins J L 1992 *Phys. Rev. B* **46** 1754
- [11] Vanderbilt D 1990 *Phys. Rev. B* **41** 7892
- [12] Monkhorst H J and Pack J D 1976 *Phys. Rev. B* **13** 5188
- [13] Vargas M C, Giannozzi P, Selloni A and Scoles G 2001 *J. Phys. Chem. B* **105** 9509
- [14] Zhang J, Chi Q, Nielsen J U, Friis E P, Andersen J E T and Ulstrup J 2000 *Langmuir* **16** 7229
- [15] Ulman A 1996 *Chem. Rev.* **96** 1965
- [16] Schreiber F 2000 *Prog. Surf. Sci.* **65** 151
- [17] Xia Y, Rogers Y A, Paul K E and Whitesides G M 1999 *Chem. Rev.* **99** 1823
- [18] Joachim C, Gimzewski J K and Aviram A 2000 *Nature* **408** 541
- [19] Cui X D, Primak A, Zarate X, Tomfohr J, Sankey O F, Moore A L, Moore T A, Gust D, Harris G and Lindsay S M 2001 *Science* **294** 571
- [20] Chi Q, Zhang J, Nielsen J U, Friis E P, Chorkendorff I, Canters G W, Andersen J E T and Ulstrup J 2000 *J. Am. Chem. Soc.* **122** 4047
- [21] Alessandrini A, Gerunda M, Canters G W, Verbeet M Ph and Facci P 2003 *Chem. Phys. Lett.* **376** 625
- [22] Kühnle A, Linderoth T R, Hammer B and Besenbacher F 2002 *Nature* **415** 891
- [23] Hayashi T, Morikawa Y and Nozoye H 2001 *J. Chem. Phys.* **114** 7615
- [24] Gottschalk J and Hammer B 2002 *J. Chem. Phys.* **116** 784
- [25] Cavalleri O, Gonella G, Terreni S, Vignolo M, Floreano L, Morgante A, Canepa M and Rolandi R 2004 *Phys. Chem. Chem. Phys.* **6** 4042
- [26] Gonella G, Terreni S, Cvetko D, Cossaro A, Mattered L, Cavalleri O, Rolandi R, Morgante A, Floreano L and Canepa M 2005 *J. Phys. Chem. B* **109** 18003
- [27] Cossaro A, Terreni S, Cavalleri O, Prato M, Cvetko D, Morgante A, Floreano L and Canepa M 2006 *Langmuir* **22** 11193

- [28] Duke C B 1996 *Chem. Rev.* **96** 1237
- [29] Hersam M C, Guisinger N P and Lyding J W 2000 *Nanotechnology* **11** 70
- [30] Zhao J and Uosaki K J 2004 *J. Phys. Chem. B* **108** 17129
- [31] Lenfant S, Krzeminski C, Delerue C, Allan G and Vuillaume D 2003 *Nano Lett.* **3** 741
- [32] Lopinski G P, Wayner D D M and Wolkow R A 2000 *Nature* **406** 48
- [33] Basu R, Guisinger N P, Greene M E and Hersam M C 2004 *Appl. Phys. Lett.* **85** 2619
- [34] Bent S F 2002 *Surf. Sci.* **500** 879
- [35] Hamers R J, Coulter S K, Ellison M D, Hovis J S, Padowitz D F, Schwartz M P, Greenlief C M and Russel J N 2000 *Acc. Chem. Rev.* **33** 617
- [36] Guisinger N P, Greene M E, Basu R, Baluch A S and Hersam M C 2004 *Nano Lett.* **4** 55
- [37] Rakshit T, Liang G-C, Ghosh A W and Datta S 2004 *Nano Lett.* **4** 1803
- [38] Ramstad A, Brocks D and Kelly P J 1995 *Phys. Rev. B* **51** 14504
- [39] Schwartz M P, Ellison M D, Coulter S K, Hovis J S and Hamers R J 2000 *J. Am. Chem. Soc.* **122** 8529
- [40] Li Q and Leung K T 2005 *J. Phys. Chem. B* **109** 1420
- [41] Hwang M J, Stockfisch T P and Hagler A T 1994 *J. Am. Chem. Soc.* **116** 2515
- [42] Ferretti A, Baldacchini C, Calzolari A, Di Felice R, Ruini A, Molinari E and Betti M G 2006 submitted